Supporting Information

Directed synthesis of $\{Cu^{II}_2Zn^{II}_2\}$ and $\{Cu^{II}_8Zn^{II}_8\}$ heterometallic complexes

María José Heras Ojea,[a] Claire Wilson,[a] Simon. J. Coles,[b] Floriana Tuna[c] and Mark Murrie[a*]

[a]*WestCHEM, School of Chemistry, University of Glasgow, University Avenue, Glasgow G12 8QQ, U.K.*

[b]*Department of Chemistry, University of Southampton, Southampton SO17 1BJ, U.K.*

[c]*School of Chemistry and Photon Science Institute, University of Manchester, Oxford Road, Manchester, M13 9PL, U.K.*

mark.murrie@glasgow.ac.uk

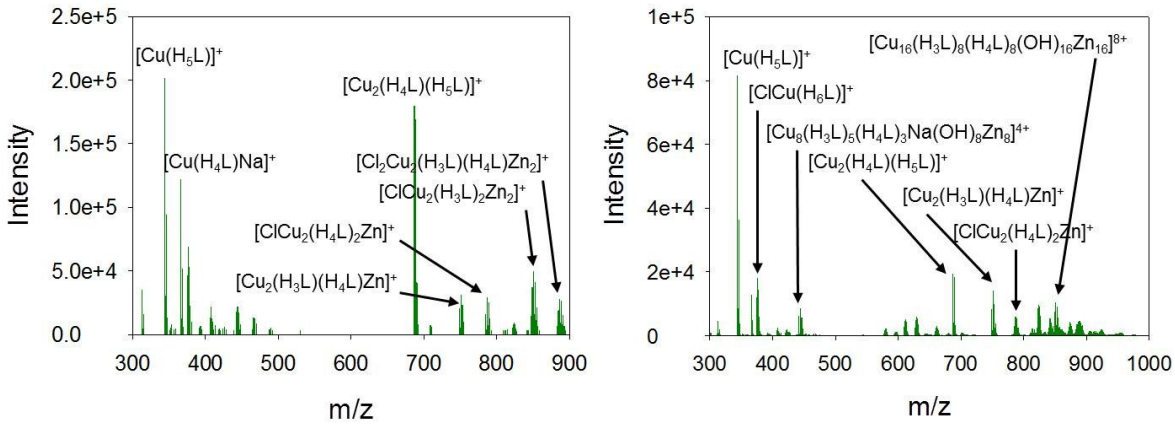

Figure S1. ESI$^+$ mass spectra for **1** (right) and **2** (left).

The majority of the peaks have been assigned considering the molecular weight and charge of the potential cations which could be present following fragmentation, and according to the tendency of H_6L to display a certain arrangement around the different metal ions. Both spectra for complexes **1** and **2** show common peaks related to a metallo-organic monomeric species ($[Cu(H_5L)]^+$) and other polynuclear complex cations containing various Cu(II) and/or Zn(II) ions ($[Cu_2(H_4L)(H_5L)]^+$, $[Cu_2(H_3L)(H_4L)Zn]^+$, $[ClCu_2(H_4L)_2Zn]^+$). Taking into account the fragmentation observed in both spectra, the central chloride in **2** could act as template to form the $\{Cu_8Zn_8\}$ ring, although assignment of the species is complicated by the presence of overlapping peaks. For **2**, the peaks observed in the region of m/z = 800-900 suggest a possible rearrangement of the $\{Cu_8Zn_8\}$ units to form a larger Cu(II)/Zn(II) complex.

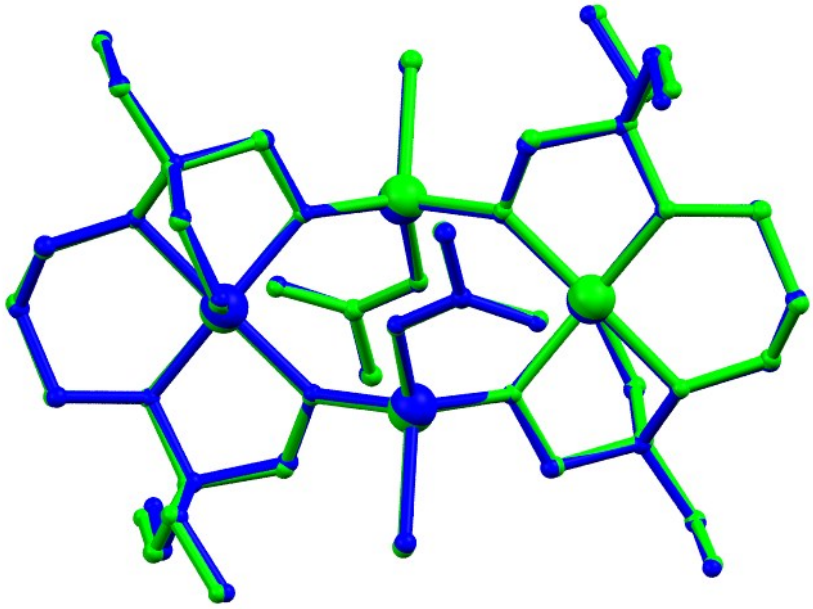

Figure S2. Overlay of the inequivalent molecules in the asymmetric unit of **1**.

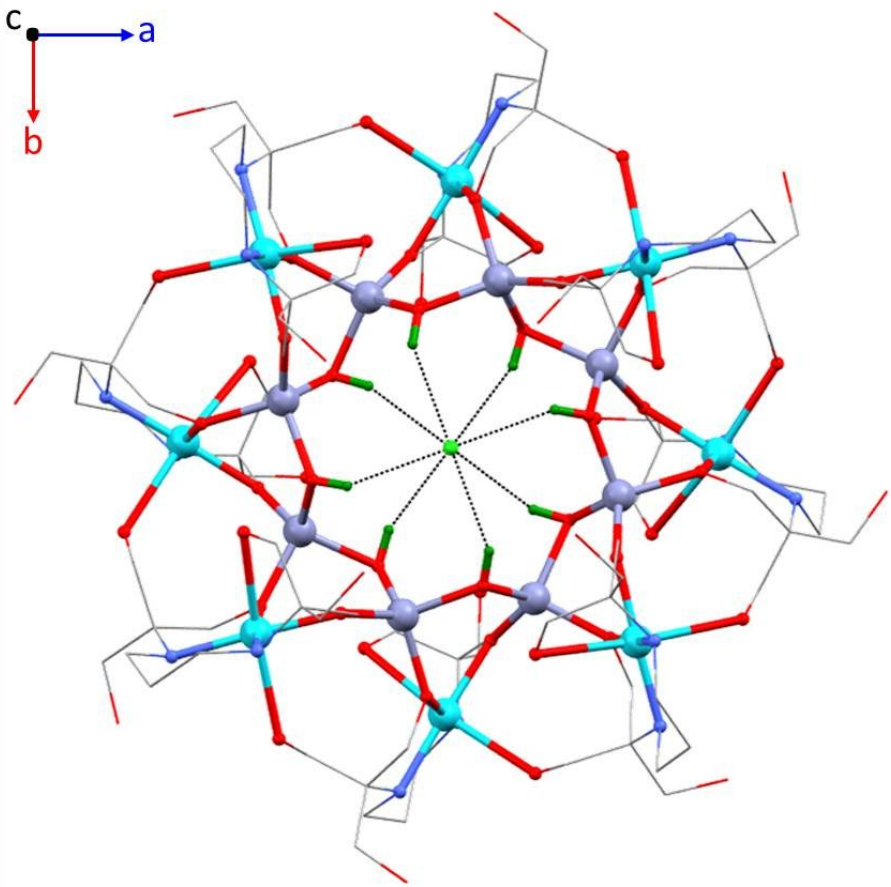

Figure S3. Intramolecular hydrogen bonding interactions in complex **2**. The hydrogen bonds between the central $Cl^{-}\cdots H(OH)$ are shown as dashed black lines. C, grey; Cl, green; Cu, turquoise; hydroxyl H atoms highlighted in dark green; N, blue; O, red; Zn, lavender.

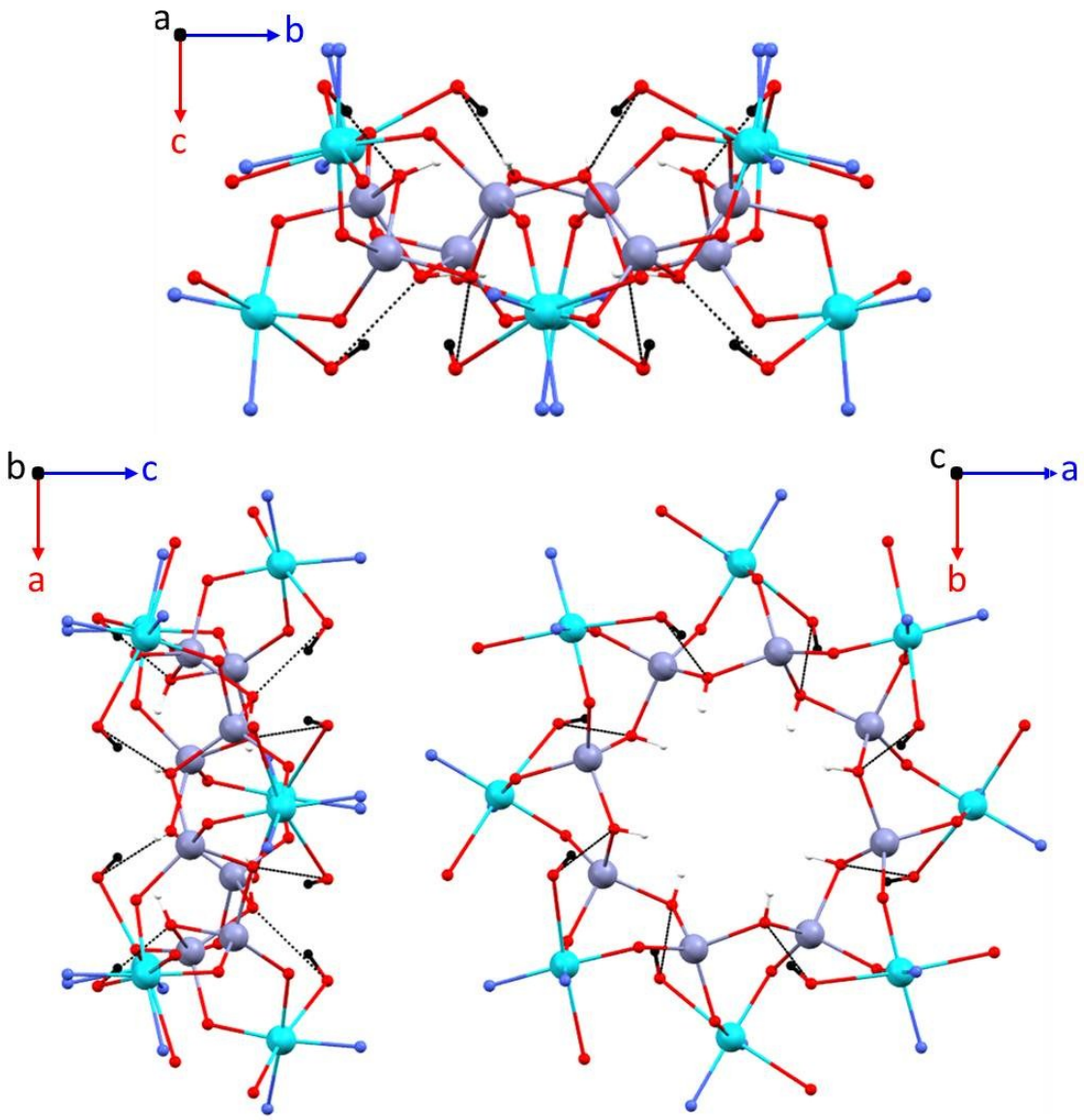

Figure S4. Intramolecular hydrogen bonding interactions in complex **2**. The hydrogen bonds between O(OH)···H(H_4L^{2-}) are shown as dashed black lines. C, grey; Cl, green; Cu, turquoise; hydroxyl H atoms highlighted in black; N, blue; O, red; Zn, lavender.

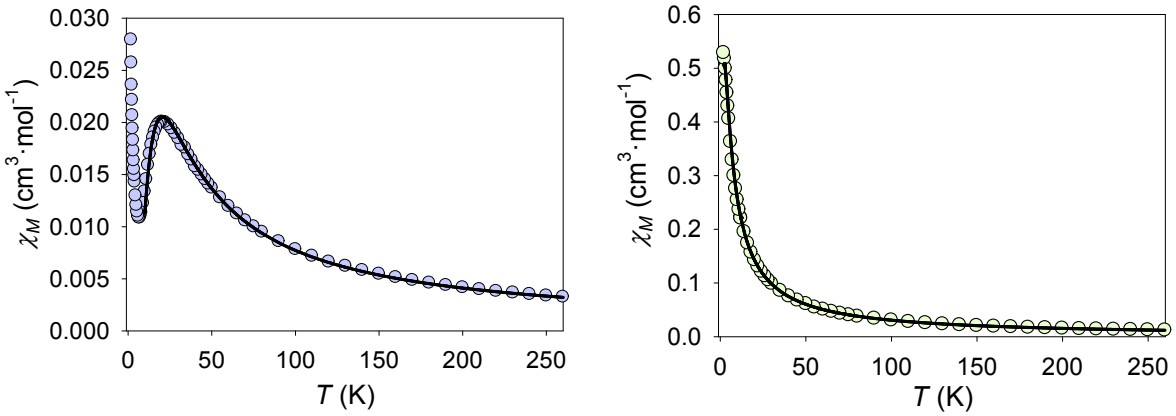

Figure S5. Molar magnetic susceptibility (χ_M) vs. temperature (T) of **1** (left) and **2** (right) in an applied field of 10000 (**1**) and 5000 (**2**) Oe. The black lines correspond to the fit.

$$H = -2J\vec{s}_1 \cdot \vec{s}_2 + g\mu_B \vec{H} \sum_{i=1}^{2} \vec{s}_i \qquad \textit{Equation S1}$$

$$H = -2J\left[\sum_{i=1}^{7} \vec{s}_i \cdot \vec{s}_{i+1} + \vec{s}_8 \cdot \vec{s}_1 \right] + g\mu_B \vec{H} \sum_{i=1}^{8} \vec{s}_i \qquad \textit{Equation S2}$$

Spin Hamiltonians used to fit the magnetic data for complexes **1** and **2**, respectively, with a single parameter J describing the exchange interaction between Cu(II) centres ($\vec{s}$ denotes the spin operator). The second term is the Zeeman interaction, with g the isotropic single-ion g factor, μ_B the Bohr magneton and H the magnetic field.

The sharp increase of the χ_M value at low temperatures in the χ_M vs. T plot for **1** indicates the presence of a small paramagnetic impurity commonly observed in this kind of system, and is in accord with the value obtained from the fit.[1, 2]

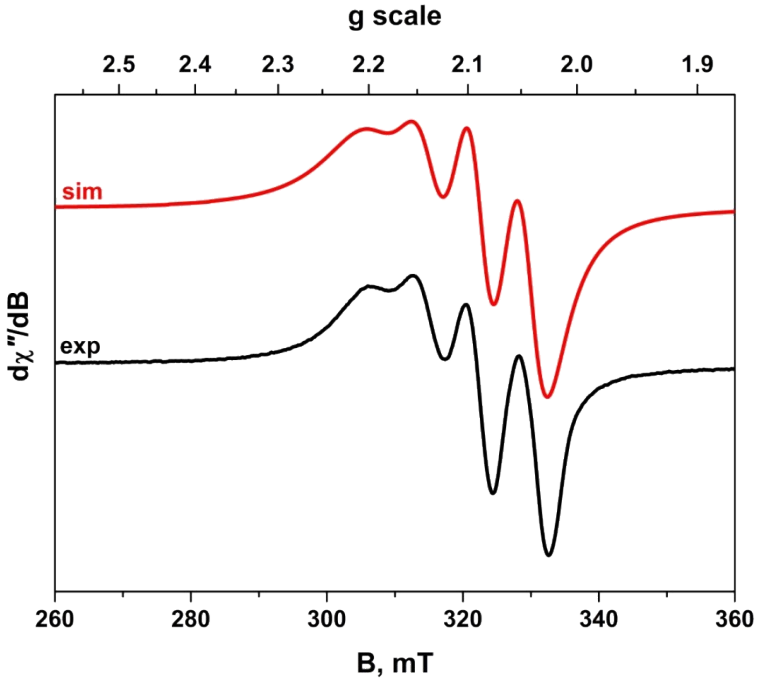

Figure S6 X-band EPR spectrum of **1** recorded in MeOH solution at 293 K (experimental conditions: frequency, 9.4269 GHz; power, 20 mW; modulation, 0.3 mT). Experimental data are represented by the black line; simulation is depicted by the red trace.

g_{iso} = 2.109

$A_{iso}\{^{63,65}Cu\} = 69 \times 10^{-4}$ cm^{-1}

Although complex **1** appears to decompose in MeOH, we assume that the g_{iso} value of the resultant Cu bis-tris propane monomeric unit should be approximately the same as the g_{iso} value for **1**.

Table S1. Selected structural parameters and coordination environments of complexes **1**, **2** and $\{Cu_2Zn_2(DEA)_4\}$.

Complex	1	2	$\{Cu_2Zn_2(DEA)_4\}$[3]
Geometry of Cu(II)	C_{4v}	D_{4h}	D_{4h}
$d_{(Cu\cdots Cua)}$ (Å)	5.724(3)	5.685(2)	5.706(9)
$d_{(Cu\cdots Zn)}$ (Å)	3.434(4)	3.389(2)	3.435(7)
$\alpha_{(Cu\cdots Zn\cdots Cua)}$ (°)	115	88.6	112.4
$\beta_{(CuOZn)}$ (°)	124.58(7)	122.52(4)	123.69(1)

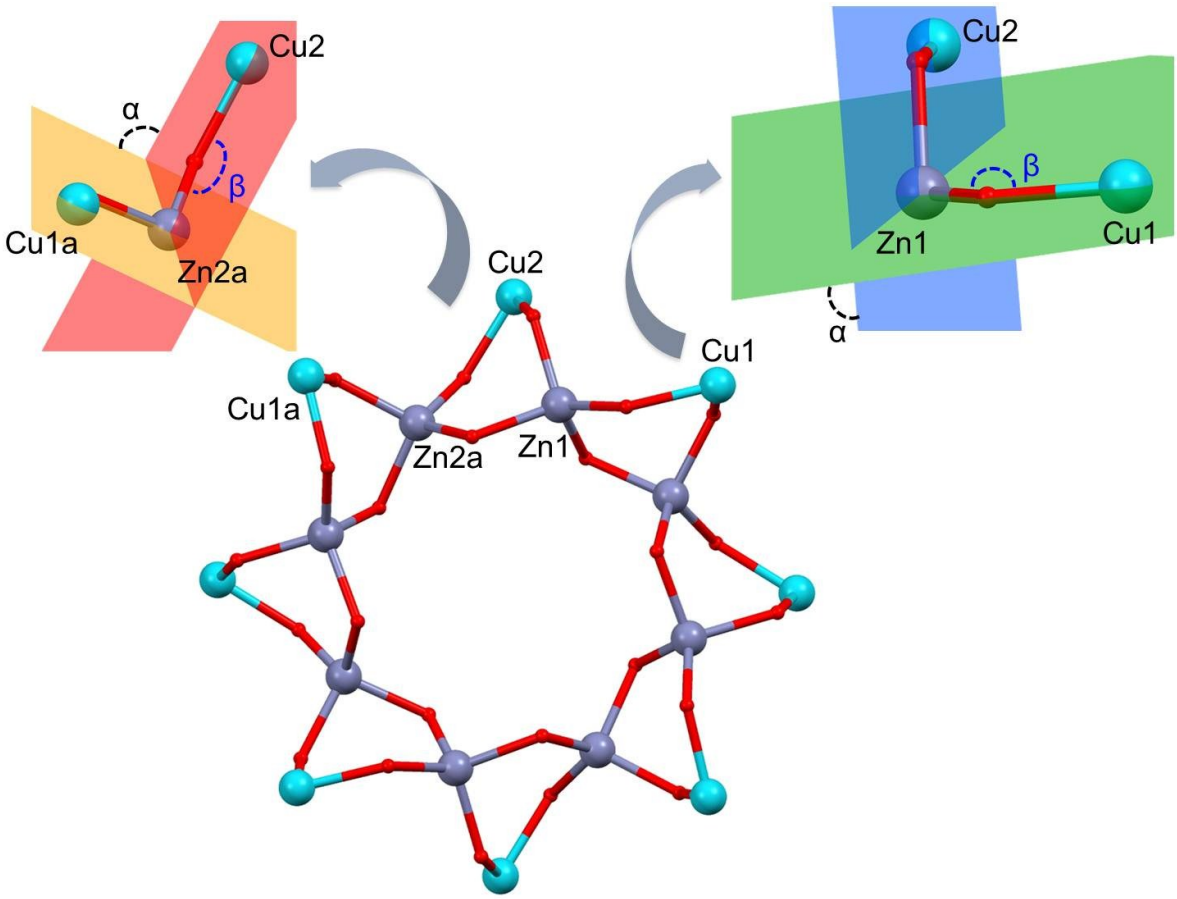

Figure S7. Detail of the crystal structure of **2**. Cu, turquoise; O, red; Zn, lavender.

References

1. O. Kahn, *Angew. Chem. Int. Ed.*, 1985, 24, 834.
2. O. Kahn, in *Advances in Inorganic Chemistry*, ed. A. G. Sykes, Academic Press, 1995, vol. 43, pp. 179.
3. E. A. Buvaylo, V. N. Kokozay, O. Y. Vassilyeva, B. W. Skelton, J. Jezierska, L. C. Brunel and A. Ozarowski, *Chem. Commun.*, 2005, 4976.